Enhanced Li-ion Transport through Selectively Solvated Ionic Layers of Single-Ion Conducting Multiblock Copolymers

Jinseok Park[a], Anne Staiger[c], Stefan Mecking[c], Karen I. Winey[a, b *]

[a]Department of Materials Science and Engineering, University of Pennsylvania, Philadelphia, Pennsylvania 19104, United States

[b]Department of Chemical and Biomolecular Engineering, University of Pennsylvania, Philadelphia, Pennsylvania 19104, United States

[c]Department of Chemistry, University of Konstanz, Universitätsstraße 10, 78457 Konstanz, Germany

Email: winey@seas.upenn.edu

TOC graphic

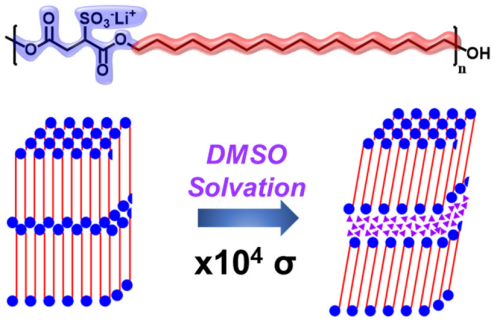

Abstract

We demonstrate enhanced Li^+ transport through the selectively solvated ionic layers of a single-ion conducting polymer. The polymer is a precisely segmented ion-containing multiblock copolymers with well-defined $Li^+SO_3^-$ ionic layers between crystallized linear aliphatic 18-carbon blocks. X-ray scattering reveals that the dimethylsulfoxide (DMSO) molecules selectively solvate the ionic layers without disrupting the crystallization of the polymer backbone. The amount of DMSO (~21 wt%) calculated from the increased layer spacing is consistent with thermogravimetric analysis. The ionic conductivity through DMSO-solvated ionic layers is > 10^4 times higher than in the dried state, indicating a significant enhancement of ion transport in the presence of this solvent. Dielectric relaxation spectroscopy (DRS) further elucidates the role of the structural relaxation time (τ) and the number of free Li^+ (n) on the ionic conductivity (σ). Specifically, DRS reveals that the solvation of ionic domains with DMSO contributes to both accelerating the structural relaxation and the dissociation of ion pairs. This study is the initial demonstration that selective solvation is a viable design strategy to improve ionic conductivity in nanophase separated, single-ion conducting multiblock copolymers.

Single-ion conducting polymer electrolytes are an important class of materials with applications in critical technologies, such as energy storage systems (e.g., batteries).[1–4] While many polymer electrolytes studied for their use in batteries are based on the classical dual-ion conducting systems of poly(ethylene oxide) (PEO) with added salt,[5] single-ion conducting polymer electrolytes have the advantage of high lithium transference numbers (t_{Li^+}), the ratio of current carried by the Li^+.[6] The t_{Li^+} is an important parameter for battery performance, because the contribution of anions to ionic conductivity limits the battery performance. For example, strong polarization induced by the mobile anions increases cell impedance and dendrite growth, which are detrimental to battery life and safety. In contrast, single-ion conducting polymer electrolytes with immobilized anions on the polymer backbone have $t_{Li^+} > 0.8$, relative to the $t_{Li^+} < 0.2$ - 0.3 of dual-ion conducting systems.[2,6] However, single-ion conducting polymer electrolytes are often limited by low ionic conductivities, due to their slow segmental dynamics of polymer chains and low concentration of free Li^+.

Adding small molecules to single-ion conducting polymer electrolytes can significantly improve the ionic conductivity due to the homogeneous plasticization of the polymer and improved ion dissociation.[7] While various gel polymer electrolytes containing small molecules typically exhibit homogenously distributed ionic groups,[8–13] fewer studies show the incorporation of small molecules into ordered nanoscale domains. For example, Kim, *et al.* reported improved anhydrous proton transport through the ionic microdomains of poly(styrene sulfonate-*b*-methylbutylene) doped with small molecules including zwitterions.[14] This improved ionic conductivity is attributed to the zwitterions increasing the local dielectric constant of the ionic domains.[14–17] In a precisely sulfonated polyethylene with nanoscale layers, Trigg, *et al.* found that upon exposition to humidity the acid layers persisted due to the polyethylene cryatllinity and the proton conductivity increased significantly.[18] These studies

suggest the potential of using small-molecule additives to selectively tune the ion channels and enhance the ionic conductivities, specifically in single-ion conducting polymer electrolytes with nanoscale morphologies.

The ionic conductivity (σ) in polymer electrolytes can be described by the Nernst-Einstein equation, $\sigma = ne^2D/(k_BT)$,[19,20] where n is the concentration of free ions, e is the number of charges carried by free ions, D is the diffusivity of ions, k_B is the Boltzmann constant, and T is the absolute temperature. The diffusivity of free ions in polymer electrolytes is typically inversely related to the polymer segmental relaxation time (τ), $D \propto 1/\tau$, assuming that the ion diffusion is controlled by the local viscosity.[19] Thus, ion transport is typically limited due to the slow segmental relaxation of the polymer chain, which is related to the glass transition temperature (T_g) of polymers.[4] The low ionic conductivity in a neat single-ion conducting polymer electrolyte is also attributed to the limited ion-pair dissociation and thus the low concentration of free ions (n).[21–23] Therefore, understanding the role of segmental dynamics and free ions is important to designing viable single-ion conducting polymer electrolytes.

In this study, we investigate the ion transport in the selectively solvated and well-defined ionic layers of a single-ion conducting polymer. The polymer matrix is a precise ion-containing multiblock copolymer containing strictly alternating lithium sulfosuccinate diester and linear aliphatic 18-carbon blocks (PES18Li). Below the melting temperature (117 °C) PES18Li self-assemblies into layered ionic domains with crystalline polyethylene blocks.[24] The large interaction parameter between the aliphatic and ionic blocks produces nanoscale phase separation with sub-3 nm domain spacings. The self-assembled ionic layers in this particular polymer are consistent with previously revealed chain-folded polymer conformations that exclude a polar functional group from a crystallizing segement in a precise polymer.[25,26]Consistent with this understanding, the ionic layers are selectively solvated by

dimethylsulfoxide (DMSO) without disrupting the crystallization of the hydrocarbon blocks, as characterized by X-ray scattering experiments. While ionic conductivity through dried ionic layers is too low to measure below 80 °C, the selective solvation of the ionic layers with DMSO significantly increases the ionic conductivity by more than 10^4 times. Also, the dielectric relaxation spectroscopy analysis reveals that the solvated ionic domains plasticized by DMSO exhibit faster structural relaxation than the dried polymer. Also, the concentration of free ions significantly increases upon solvation with DMSO. Specifically, at 340 K, the number of free ions contributing to the ionic conductivity in the solvated PES18Li is ~ 27 times larger than the dried PES18Li. This initial study establishes the broad ability to enhance cation transport by selectively solvating the ionic nanodomains within single-ion conducting ordered multiblock copolymers.

The synthesis of the PES18Li multiblock copolymer and its basic characterization including ^{1}H NMR, gel permeation chromatography, differential scanning calorimetry, and temperature-dependent morphologies in dried PES18Li polymers were reported previously.[24,27,28] The polymer molecular weight determined by the ^{1}H NMR end-group analysis was 7.7 kg/mol, which corresponds to ~17 repeating subunits. This paper further elaborates on the characterization of morphology and ion transport in dried and solvated PES18Li. The details of sample preparation and characterization procedures are described in the Supporting Information.

X-ray scattering compares the morphology of dried and solvated PES18Li (**Figure 1a**). For the dried sample, the ratio of q^*:$2q^*$ at $q < 0.8$ Å^{-1} is consistent with the assembly of ionic layers, which coexist with the semicrystalline feature at $q \sim 1.5$ Å^{-1} corresponding to polyethylene (PE) crystals with hexagonal symmetry.[29] The coexistence of ionic layers and crystalline PE is illustrated schematically in **Figure 1b**. In the dried sample, the layer spacing

of 31.4 Å is larger than the length of the all-*trans* 18-carbons (21.4 Å), accounting for the two polar groups in the layered assembly. The difference between these lengths is consistent with the size and volume fraction (0.31) of the polar blocks, indicating that the linear aliphatic blocks are nominally perpendicular to the ionic layers. This perpendicular orientation was also observed in grazing incidence X-ray scattering experiments.[30]

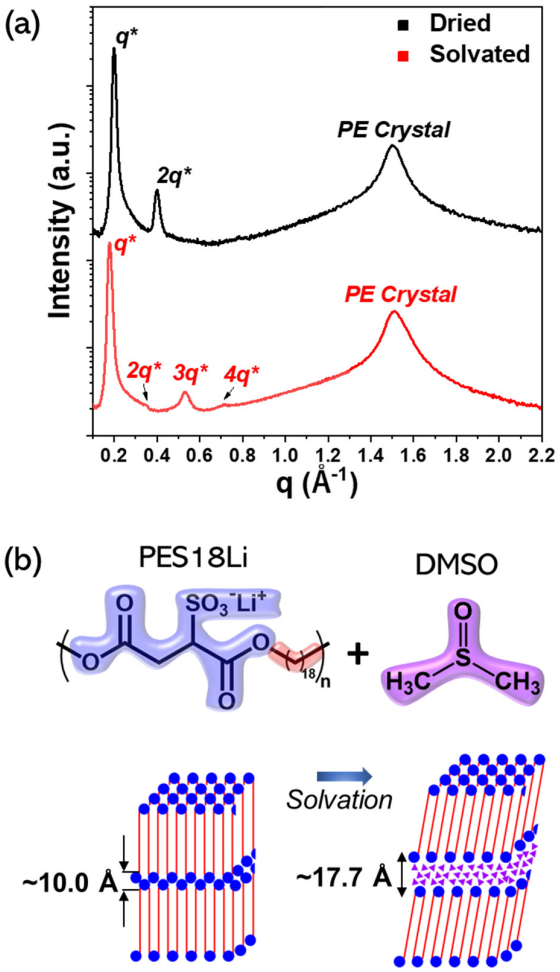

Figure 1. (a) X-ray scattering profiles of dried (black) and solvated (red) samples. The q* ratios at $q < 0.8$ Å^{-1} are labeled for the layered assembly of polar ionic domains. The peak at $q \sim 1.5$ Å^{-1} corresponds to the (100) reflection of hexagonal polyethylene-like crystals. (b) Schematics of chain conformation before and after the solvation of PES18Li, showing the selective solvation of polar ionic domains (blue circles) with the DMSO molecules (purple triangles).

The solvated PES18Li film is prepared by dissolving PES18Li in DMSO followed by solvent casting, see Supporting Information for the detailed procedure. Thermogravimetric analysis (TGA) indicates ~ 21 wt% DMSO in the solvated film (**Figure S1**). X-ray scattering of the solvated sample indicates that the distance between the ionic layers increases from 31.4 to 35.4 Å as calculated from q^*, while the semicrystalline feature at $q \sim 1.5$ Å^{-1} is maintained. The odd-numbered peaks of the ionic layers at $q < 0.8$ Å^{-1} exhibit strong reflections, whereas the even-numbered peaks are significantly diminished. We attributed this to the volumetrically symmetric polar and non-polar regions in the solvated sample, in which the volume fraction (f_p) of solvated polar domains is nearly 0.50 compared to 0.31 of the dried sample. The decrease of even-number scattering peaks of layered morphologies has been observed in volumetrically symmetric AB diblock and $(AB)_n$ multiblock copolymers.[31–33] By assuming $f_p = 0.50$ and all *trans* conformations of the linear aliphatic blocks, the tilt angle of the hydrocarbon chain relative to the solvated ionic layers is calculated as ~ 34 °, **Figure S2**. The total thickness of the polar domain is 17.7 Å of which ~ 10 Å can be attributed to the polar blocks and the remainder (~ 7.7 Å) is occupied by DMSO. This corresponds to a volume fraction of DMSO ~ 0.22, which is consistent with the TGA results. The selective solvation of the polar domains with DMSO molecules during solvent casting is attributed to an ultrahigh interaction parameter (χ) between the polar ionic and non-polar hydrocarbon blocks. Note that we previously reported $\chi = \sim 3.16$ at 100 °C (reference volume of 118 Å^3) for a multiblock copolymer with the same polar block chemistry and a shorter 12-carbon aliphatic block.[24] Upon solvation, DMSO molecules preferentially and strongly interact with the polar domains rather than the non-polar aliphatic blocks, thereby permitting the PES18Li polymer to crystallize. Importantly, within these the semicrystalline polymer matrix, DMSO selectively solvates well-defined ionic nanolayers < 2 nm thick that define the conductive pathways. The quantity of solvent could be

used to tune the thickness of these conductive layers.

The ionic conductivities of dried and solvated PES18Li are shown in **Figure 2**. The ionic conductivity of the dried sample is only measurable at temperatures > ~ 80 °C, due to the low ionic conductivity at lower temperatures. The ionic conductivity of the dried sample was measured upon cooling and exhibits an increase of ionic conductivity at the morphology transition from hexagonally packed cylinders (HEX) to double gyroid (GYR) ionic domains, as previous reported.[24] The ionic conductivity increases ~10-fold at the HEX to GYR order-to-order transition, and this is attributed to the bicontinuous ionic domains of GYR. The ionic conductivities of the solvated sample were measured at ~ 30 - 70 °C to prevent the evaporation of DMSO and found to be reproducible throughout 4 cycles of heating and cooling (**Figure S3**). The ionic conductivity of the solvated sample in the layered morphology is ~ 10^{-6} S/cm at ~ 70 °C, which is more than 10^4 times higher than in the dried sample (~ 80 °C). The selective solvation of the ionic layers in PES18Li with DMSO results in a significant increase in ionic conductivity relative to the dried polymer.

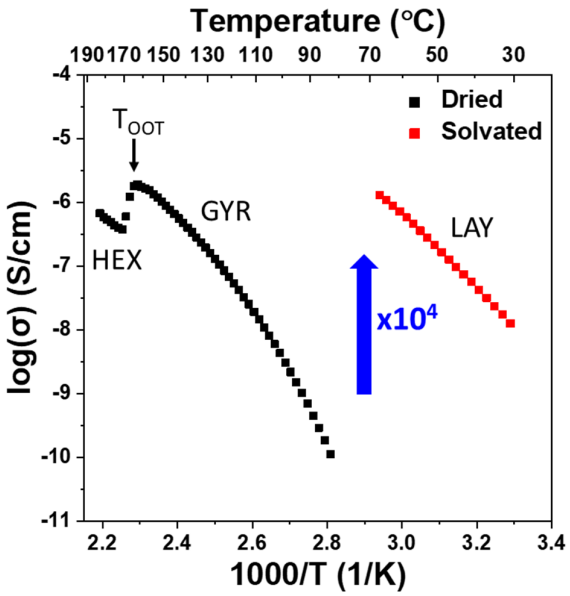

Figure 2. Ionic conductivity of dried (black) and solvated (red) samples as a function of temperature upon cooling. For the dried sample, T_{OOT} indicates the order-to-order transition temperature determined from differential scanning calorimetry upon cooling. HEX and GYR indicate the hexagonally packed cylinder and double gyroid ionic aggregate morphologies, respectively. For the solvated sample, LAY indicates the layered ionic domains.

The dielectric responses of both samples are further analyzed to elucidate the origins of the higher ionic conductivity when solvated. The imaginary part of the permittivity (ε") provides the dc conductivity, which is consistent with the conductivity determined from the Nyquist plot. The real part of the permittivity (ε') fit to the Havrilirak-Negami equation provides the structural relaxation time (τ) in dried and solvated PES18Li.[19,34,35] An example of this fit is provided in **Figure S4**. The range of τ in solvated sample measured at 304 – 340 K is comparable to the range of τ in dried sample measured at 360 – 416 K (**Figure 3a**). For the dried sample, the values of τ are well described by the Vogel-Fulcher-Tamman (VFT) relationship, where the glass transition temperature (T_g) determined from the DSC (~ 58 °C) corresponds to τ ~ 150 sec. This is consistent with the typical τ of 100 – 1000 sec at T_g.[35,36] The VFT relationship of the solvated sample indicates that the temperature at τ of 100 – 1000 is ~

-25 °C. Faster structural relaxations in the solvated sample are evident from the temperature-dependent τ, and are readily attributed to the lower local viscosity in the solvated ionic domains relative to the dried domains. Thus, the selective solvation with DMSO plasticizes and increases the structural relaxation rate of ionic layers.

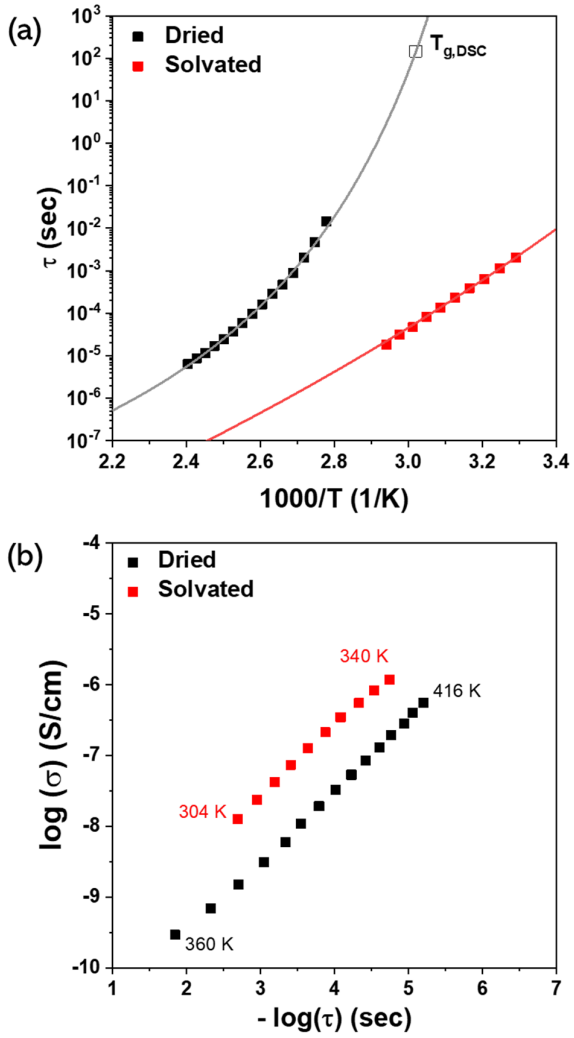

Figure 3. (a) Structural relaxation times (τ, symbols) and the VFT fits (lines) of dried (black) and solvated (red) PES18Li as a function of temperature. The τ values are obtained from the real part of permittivity as described in the text. $T_{g,DSC}$ of dried sample was reported in reference.[24] (b) Ionic conductivities as a function of τ.

The ionic conductivities of dried and solvated PES18Li are shown as a function of τ (**Figure 3b**). The ionic conductivity of the solvated sample is higher than the dried sample at the same structural relaxation time, and this indicates that the factors contributing to the higher ionic conductivity in the solvated sample include more than the faster structural relaxations of the solvated ionic domains. Considering the Nernst-Einstein equation, $\sigma \sim nD \propto n/\tau$, a higher free-ion concentration (n) and faster free ion diffusion (D) might also contribute to the higher ionic conductivity through solvated domains. Specifically, the polar DMSO molecules promote dissociation of Li^+ from the $Li^+SO_3^-$ ion pairs to increase the number of charge carriers. This insight is further supported by plotting the molar ionic conductivities (σ/n_o) and comparing them with the ideal Walden line, **Figure S5**. The Walden rule indicates that the molar ionic conductivity is inversely proportional to the viscosity of an electrolyte.[37] While dried PES18Li shows ideal Walden behavior, solvated PES18Li exhibits superionic behavior with more than an order of magnitude increase of ionic conductivity relative to the ideal line.[17,38]

Figure 4a shows the diffusion coefficients of free ions (D) as obtained from the Macdonald-Trukhan model (see Supporting Information).[19,20,39,40] By comparing with Figure 2, notice that D in the dried PES18Li at 416 K is ~ 10 times higher than D in the solvated PES18Li at 340 K, while the conductivity of the dried sample at 416 K is slightly lower than the solvated sample at 340 K. This strongly indicates that the solvated PES18Li has more free ions despite the lower temperature (ΔT = 76 K). The number of free ions (n) in the dried and solvated samples was calculated from the relationship $n = \sigma k_B T/(D e^2)$ and n exhibit Arrhenius temperature dependence; $n = n_\infty \exp(-E_a/k_B T)$. (**Figure 4b**).[39,41] The number density of free ions in the dried PES18Li is independent of temperature, indicating that the strongly attractive ionic groups prevent dissociation of ion pairs to free Li^+ ions in the dry condition, while the incorporation of DMSO exhibits a temperature dependence on n. The ratio of the number

density of free ions at infinite temperature (n_∞) relative to the number density of total available ions (n_o) in the system provides the fraction of ions that contribute to the ionic conductivity.[22,23,42] The value of n_o is calculated from the van der Waals volume. The ratio of n_∞/n_o for dried and solvated PES18Li is 0.00125 and 0.299, respectively, indicating that the fraction of free ions contributing to the ionic conductivity in the solvated polymer is ~ 240 times larger than the dried polymer at infinite temperature. At 340 K, the fraction of free ions increases by 27 times when solvated with DMSO. Clearly, DMSO selectively solvates the nanoscale ionic layers, promotes structural relaxations for faster ion diffusion, and dissociates more Li^+ ions compared to the dry polymer, leading to higher ionic conductivity.

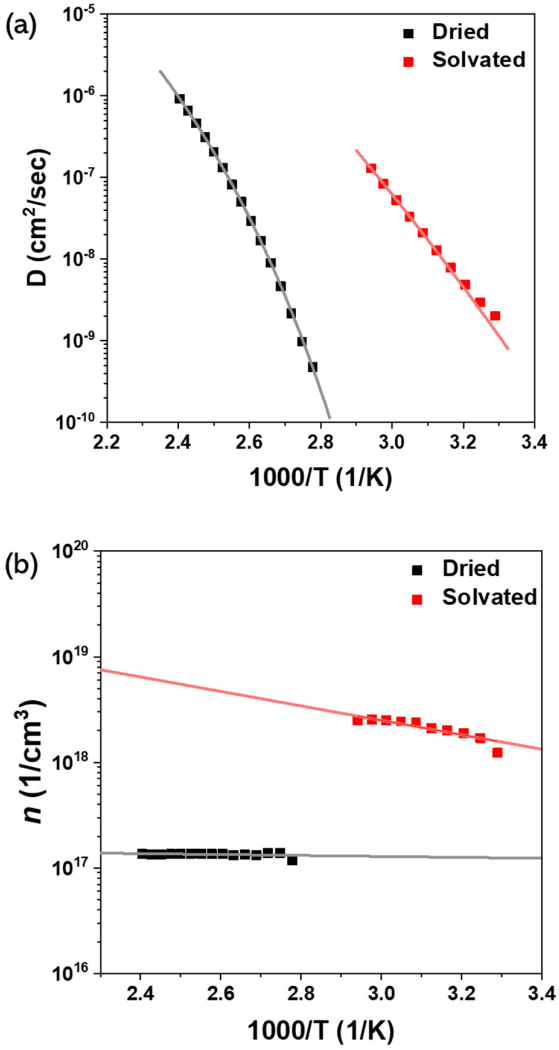

Figure 4. (a) Diffusion coefficients of free ions (D, symbols) and VFT fits (lines) of dried (black) and solvated (red) PES18Li as a function of temperature. (b) The number density of free ions (*n*, symbols) and Arrhenius fits (lines) of dried (black) and solvated (red) PES18Li as a function of temperature.

To elucidate the ionic conductivity contributed by the free ions, the true molar ionic conductivities ($\Lambda = \sigma/n$) of dried and solvated polymers are shown as a function of τ (**Figure 5**). The true molar ionic conductivities of the two systems are comparable, unlike the apparent (**Figure 3b**) and molar ionic conductivities (**Figure S5)**. Note that **Figure S5** presents the ionic conductivity normalized by the total number density of ions (σ/n_o), which assumes the full

dissociation of ion pairs. The similarity in Λ for the dried and solvated polymers indicates that the observed differences in σ are dominated by differences in n, thus highlighting the importance of ion dissociation by the polar solvent. Also, the true molar conductivities of Λ in both samples fall in the superionic regime relative to the ideal Walden plot (purple line, slope 1), demonstrating a strong decorrelation between the ion transport and structural relaxation rate.[19] We attribute the superionic behavior of free ions in both dried and solvated samples to Li^+ hopping, where the rate of ion jump within the ionic domains is much faster than segmental dynamics. In **Figure 5**, the solvated polymer has a slope of 0.85 due to n increasing with temperature, while the dry polymer has a slope of 1.00 consistent with a temperature-independent n (**Figure 4b**). The apparent ionic conductivity (σ) and molar ionic conductivity (σ/n_o) in both samples exhibit slopes of 1.00 (**Figure 3** and **Figure S5**). Therefore, **Figure 5** highlights the importance of the number of free ions in understanding the temperature-dependent ionic conductivities in these single-ion conductors.

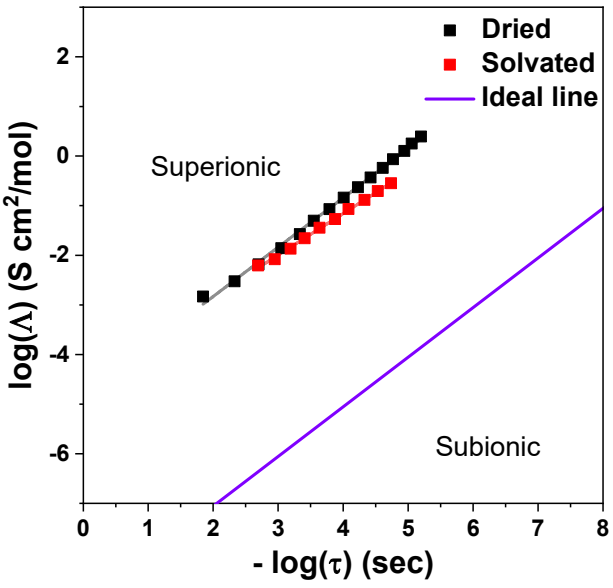

Figure 5. The true molar conductivities ($\Lambda = \sigma/n$) of dried (black) and solvated (red) PES18Li as a function of the structural relaxation time. The slope of lines for dried and solvated samples are 1.00 and 0.85, respectively. The purple line is the ideal Walden line with a slope of 1.00.

In summary, we demonstrate the role of structural relaxation and the number of free ions on the improved ionic conductivity in a solvated and ordered single-ion conducting polymer. The precise ion-containing multiblock copolymer, poly(octadecanediyl-*alt*-lithium sulfosuccinate diester), forms nanoscale ionic layers selectively solvated with DMSO molecules. The dielectric relaxation spectroscopy reveals that the increase of ionic conductivities in the solvated polymer is due to faster structural relaxations and higher concentrations of free ions. Both samples exhibit superionic ion transport as compared to the classical Walden behavior. This initial study clearly demonstrates the value of incorporating a polar solvent to modify the ordered ionic nanodomains of single-ion conducting multiblock copolymers and to improve ionic conductivity. Further improvements to the ionic conductivity of these multiblock copolymers might be achieved by selecting alternative combinations of functional groups on the polymer and solvents, and by solvating other ordered morphologies such as double gyroid.

ASSOCIATED CONTENT

Supporting Information

Expermental section including DRS analysis, thermogravimetric analysis, schematics for polymer chain structures, ionic conductivity of PES18Li_DMSO upon cycling, an example of storage permittivity and fit, molar ionic conductivity.

AUTHOR INFORMATION

Corresponding Author

Karen I. Winey − Department of Materials Science and Engineering, Department of Chemical and Biomolecular Engineering, University of Pennsylvania, Philadelphia, Pennsylvania 19104, United States. orcid.org/0000-0001-5856-3410; Email: winey@seas.upenn.edu

Authors

Jinseok Park − Department of Materials Science and Engineering, University of Pennsylvania, Philadelphia, Pennsylvania 19104, United States; orcid.org/0000-0002-0389-9707

Anne Staiger − Department of Chemistry, University of Konstanz, 78457 Konstanz, Germany; orcid.org/0000-0002-6103-4402

Stefan Mecking − Department of Chemistry, University of Konstanz, 78457 Konstanz, Germany; orcid.org/0000-0002-6618-6659

ACKNOWLEDGMENTS

J.P. and K.I.W. acknowledge funding by the NSF DMR (1904767). J.P. and K.I.W. also acknowledge NSF MRSEC (17-20530), NSF MRI (17-25969), and ARO DURIP grant (W911NF-17-1-0282) for the Dual Source and Environmental X-ray Scattering facility at the University of Pennsylvania. Funding by the Baden-Württemberg Foundation (project 'PRICON') is gratefully acknowledged.

References

(1) Zhang, H.; Li, C.; Piszcz, M.; Coya, E.; Rojo, T.; Rodriguez-Martinez, L. M.; Armand, M.; Zhou, Z. Single Lithium-Ion Conducting Solid Polymer Electrolytes: Advances and Perspectives. *Chem. Soc. Rev.* **2017**, *46*, 797–815.

(2) Bocharova, V.; Sokolov, A. P. Perspectives for Polymer Electrolytes: A View from Fundamentals of Ionic Conductivity. *Macromolecules* **2020**, *53*, 4141–4157.

(3) Zhu, J.; Zhang, Z.; Zhao, S.; Westover, A. S.; Belharouak, I.; Cao, P. F. Single-Ion Conducting Polymer Electrolytes for Solid-State Lithium–Metal Batteries: Design, Performance, and Challenges. *Adv. Energy Mater.* **2021**, *11*, 1–18.

(4) Mogurampelly, S.; Borodin, O.; Ganesan, V. Computer Simulations of Ion Transport in Polymer Electrolyte Membranes. *Annu. Rev. Chem. Biomol. Eng.* **2016**, *7*, 349–371.

(5) Xue, Z.; He, D.; Xie, X. Poly(Ethylene Oxide)-Based Electrolytes for Lithium-Ion Batteries. *J. Mater. Chem. A* **2015**, *3*, 19218–19253.

(6) Diederichsen, K. M.; McShane, E. J.; McCloskey, B. D. Promising Routes to a High Li+ Transference Number Electrolyte for Lithium Ion Batteries. *ACS Energy Lett.* **2017**, *2*, 2563–2575.

(7) Chen, Q.; Bao, N.; Wang, J. H. H.; Tunic, T.; Liang, S.; Colby, R. H. Linear Viscoelasticity and Dielectric Spectroscopy of Ionomer/Plasticizer Mixtures: A Transition from Ionomer to Polyelectrolyte. *Macromolecules* **2015**, *48*, 8240–8252.

(8) Cheng, X.; Pan, J.; Zhao, Y.; Liao, M.; Peng, H. Gel Polymer Electrolytes for Electrochemical Energy Storage. *Adv. Energy Mater.* **2018**, *8*, 1–16.

(9) Porcarelli, L.; Shaplov, A. S.; Bella, F.; Nair, J. R.; Mecerreyes, D.; Gerbaldi, C. Single-Ion Conducting Polymer Electrolytes for Lithium Metal Polymer Batteries That Operate at Ambient Temperature. *ACS Energy Lett.* **2016**, *1*, 678–682.

(10) Nguyen, H. D.; Kim, G. T.; Shi, J.; Paillard, E.; Judeinstein, P.; Lyonnard, S.; Bresser, D.; Iojoiu, C. Nanostructured Multi-Block Copolymer Single-Ion Conductors for Safer High-Performance Lithium Batteries. *Energy Environ. Sci.* **2018**, *11*, 3298–3309.

(11) Lu, Q.; He, Y.-B.; Yu, Q.; Li, B.; Kaneti, Y. V.; Yao, Y.; Kang, F.; Yang, Q.-H. Dendrite-Free High-Rate Long-Life Lithium Metal Batteries with a 3D Cross-Linked Network.Pdf. *Adv. Mater.* **2017**, *29*, 1604460.

(12) Oh, H.; Xu, K.; Yoo, H. D.; Kim, D. S.; Chanthad, C.; Yang, G.; Jin, J.; Ayhan, I. A.; Oh, S. M.; Wang, Q. Poly(Arylene Ether)-Based Single-Ion Conductors for Lithium-Ion Batteries. *Chem. Mater.* **2016**, *28*, 188–196.

(13) Rohan, R.; Pareek, K.; Chen, Z.; Cai, W.; Zhang, Y.; Xu, G.; Gao, Z.; Cheng, H. A High Performance Polysiloxane-Based Single Ion Conducting Polymeric Electrolyte Membrane for Application in Lithium Ion Batteries. *J. Mater. Chem. A* **2015**, *3*, 20267–20276.

(14) Kim, O.; Kim, K.; Choi, U. H.; Park, M. J. Tuning Anhydrous Proton Conduction in Single-Ion Polymers by Crystalline Ion Channels. *Nat. Commun.* **2018**, *9*, 1–8.

(15) Tiyapiboonchaiya, C.; Pringle, J. M.; Sun, J.; Byrne, N.; Howlett, P. C.; MacFarlane, D. R.; Forsyth, M. The Zwitterion Effect in High-Conductivity Polyelectrolyte Materials. *Nat. Mater.* **2004**, *3*, 29–32.

(16) Mei, W.; Rothenberger, A. J.; Bostwick, J. E.; Rinehart, J. M.; Hickey, R. J.; Colby, R. H. Zwitterions Raise the Dielectric Constant of Soft Materials. *Phys. Rev. Lett.* **2021**, *127*, 228001.

(17) Jones, S. D.; Nguyen, H.; Richardson, P. M.; Chen, Y. Q.; Wyckoff, K. E.; Hawker, C. J.; Clément, R. J.; Fredrickson, G. H.; Segalman, R. A. Design of Polymeric Zwitterionic Solid Electrolytes with Superionic Lithium Transport. *ACS Cent. Sci.* **2022**, *8*, 169–175.

(18) Trigg, E. B.; Gaines, T. W.; Maréchal, M.; Moed, D. E.; Rannou, P.; Wagener, K. B.; Stevens, M. J.; Winey, K. I. Self-Assembled Highly Ordered Acid Layers in Precisely Sulfonated Polyethylene Produce Efficient Proton Transport. *Nat. Mater.* **2018**, *17*, 725–731.

(19) Wang, Y.; Fan, F.; Agapov, A. L.; Saito, T.; Yang, J.; Yu, X.; Hong, K.; Mays, J.; Sokolov, A. P. Examination of the Fundamental Relation between Ionic Transport and Segmental Relaxation in Polymer Electrolytes. *Polymer (Guildf).* **2014**, *55*, 4067–4076.

(20) Pal, P.; Ghosh, A. Broadband Dielectric Spectroscopy of BMPTFSI Ionic Liquid Doped Solid-State Polymer Electrolytes: Coupled Ion Transport and Dielectric Relaxation Mechanism. *J. Appl. Phys.* **2020**, *128*.

(21) Fragiadakis, D.; Dou, S.; Colby, R. H.; Runt, J. Molecular Mobility, Ion Mobility and Mobile Ion Concentration in Polyethylene Oxide-Based Polyurethane Ionomers. *Macromolecules* **2008**, *41*, 5723–5728.

(22) Lee, M.; Choi, U. H.; Colby, R. H.; Gibson, H. W. Ion Conduction in Imidazolium Acrylate Ionic Liquids and Their Polymers. *Chem. Mater.* **2010**, *22*, 5814–5822.

(23) Choi, U. H.; Ye, Y.; Salas De La Cruz, D.; Liu, W.; Winey, K. I.; Elabd, Y. A.; Runt, J.; Colby, R. H. Dielectric and Viscoelastic Responses of Imidazolium-Based Ionomers with Different Counterions and Side Chain Lengths. *Macromolecules* **2014**, *47*, 777–790.

(24) Park, J.; Staiger, A.; Mecking, S.; Winey, K. I. Sub-3-Nanometer Domain Spacings of Ultrahigh-χ Multiblock Copolymers with Pendant Ionic Groups. *ACS Nano* **2021**, *15*, 16738–16747.

(25) Trigg, E. B.; Stevens, M. J.; Winey, K. I. Chain Folding Produces a Multilayered Morphology in a Precise Polymer: Simulations and Experiments. *J. Am. Chem. Soc.* **2017**, *139*, 3747–3755.

(26) Trigg, E. B.; Middleton, L. R.; Moed, D. E.; Winey, K. I. Transverse Orientation of Acid Layers in the Crystallites of a Precise Polymer. *Macromolecules* **2017**, *50*, 8988–8995.

(27) Yan, L.; Rank, C.; Mecking, S.; Winey, K. I. Gyroid and Other Ordered Morphologies in Single-Ion Conducting Polymers and Their Impact on Ion Conductivity. *J. Am. Chem. Soc.* **2020**, *142*, 857–866.

(28) Park, J.; Staiger, A.; Mecking, S.; Winey, K. I. Structure-Property Relationships in Single-Ion Conducting Multiblock Copolymers: A Phase Diagram and Ionic

Conductivities. *Macromolecules* **2021**, *54*, 4269–4279.

(29) Tsubakihara, S.; Nakamura, A.; Yasuniwa, M. Hexagonal Phase of Polyethylene Fibers under High Pressure. *Polym. J.* **1991**, *23*, 1317–1324.

(30) Park, J.; Staiger, A.; Mecking, S.; Winey, K. I. Ordered Nanostructures in Thin Films of Precise Ion-Containing Multiblock Copolymers. *ACS Cent. Sci.* **2022**, *8*, 388–393.

(31) Bendejacq, D.; Ponsinet, V.; Joanicot, M.; Loo, Y. L.; Register, R. A. Well-Ordered Microdomain Structures in Polydisperse Poly(Styrene)-Poly(Acrylic Acid) Diblock Copolymers from Controlled Radical Polymerization. *Macromolecules* **2002**, *35*, 6645–6649.

(32) Wu, L.; Cochran, E. W.; Lodge, T. P.; Bates, F. S. Consequences of Block Number on the Order-Disorder Transition and Viscoelastic Properties of Linear (AB) n Multiblock Copolymers. *Macromolecules* **2004**, *37*, 3360–3368.

(33) Steube, M.; Johann, T.; Galanos, E.; Appold, M.; Rüttiger, C.; Mezger, M.; Gallei, M.; Müller, A. H. E.; Floudas, G.; Frey, H. Isoprene/Styrene Tapered Multiblock Copolymers with up to Ten Blocks: Synthesis, Phase Behavior, Order, and Mechanical Properties. *Macromolecules* **2018**, *51*, 10246–10258.

(34) Kremer, F.; Schönhals, A. *Broadbank Dielectric Spectroscopy*; Springer Science & Business Media: Berlin, 2002.

(35) Fan, F.; Wang, Y.; Hong, T.; Heres, M. F.; Saito, T.; Sokolov, A. P. Ion Conduction in Polymerized Ionic Liquids with Different Pendant Groups. *Macromolecules* **2015**, *48*, 4461–4470.

(36) Tudryn, G. J.; O'Reilly, M. V.; Dou, S.; King, D. R.; Winey, K. I.; Runt, J.; Colby, R. H. Molecular Mobility and Cation Conduction in Polyether-Ester-Sulfonate Copolymer Ionomers. *Macromolecules* **2012**, *45*, 3962–3973.

(37) Walden, P. Über Organische Lösungs- Und Ionisierungsmittel: III. Teil: Innere Reibung Und Deren Zusammenhang Mit Dem Leitvermögen. *Zeitschrift für Phys. Chemie* **1906**, *55U*, 207–249.

(38) Wang, Y.; Fan, F.; Agapov, A. L.; Yu, X.; Hong, K.; Mays, J.; Sokolov, A. P. Design of Superionic Polymers - New Insights from Walden Plot Analysis. *Solid State Ionics* **2014**, *262*, 782–784.

(39) Pal, P.; Ghosh, A. Ion Conduction and Relaxation Mechanism in Ionogels Embedded with Imidazolium Based Ionic Liquids. *J. Appl. Phys.* **2019**, *126*, 135102.

(40) Pal, P.; Ghosh, A. Ion Transport and Segmental Dynamics in Cross-Linked Poly(Ethylene Glycol) Diacrylate-Based Solid-like Polymer Electrolytes. *J. Phys. Chem. C* **2022**, *126*, 4799–4806.

(41) Wang, Y.; Sun, C. N.; Fan, F.; Sangoro, J. R.; Berman, M. B.; Greenbaum, S. G.; Zawodzinski, T. A.; Sokolov, A. P. Examination of Methods to Determine Free-Ion Diffusivity and Number Density from Analysis of Electrode Polarization. *Phys. Rev. E - Stat. Nonlinear, Soft Matter Phys.* **2013**, *87*, 1–9.

(42) Choi, U. H.; Lee, M.; Wang, S.; Liu, W.; Winey, K. I.; Gibson, H. W.; Colby, R. H. Ionic Conduction and Dielectric Response of Poly(Imidazolium Acrylate) Ionomers.

Macromolecules **2012**, *45*, 3974–3985.